THERMAL ANALYSIS OF CIRCULAR ANNULAR CONFIGURATIONS WITH DISTRIBUTED HEAT SOURCES

by

J.R. Culham[1] and M.M. Yovanovich[2]
Microelectronics Heat Transfer Laboratory
University of Waterloo
Waterloo, Ontario, Canada N2L 3G1

and

K.D. Graham[3]
Northern Telecom Limited
Ottawa, Ontario, Canada K2H 8V4

ABSTRACT

The heat transfer process in selected regions of microelectronic circuit boards, such as in the vicinity of a through via or in an omni-directional fin can be modelled as a circular annular fin (CAF). An analytical model is presented for predicting the temperature distribution in CAF's with distributed sources, given a minimum of basic design information such as thermal conductivities, heat source strengths and locations and heat transfer coefficients.

Three typical microelectronic examples are discussed to show the sensitivity of the model to changes in design parameters and a general method is presented for determining temperature profiles in single source applications.

Accurate and efficient BASIC routines, which can be used to compute the modified Bessel functions used in the analytic solution, are presented in detail.

NOMENCLATURE

	- inner radius of the i'th element, m
A	- surface area, m^2
b_i	- outer radius of the i'th element, m
b_N	- overall outer radius, m
Bi	- Biot number, ht/k_e
C_1, C_2, etc.	- constants of integration
h	- film coefficient, W/m^2K
I_0	- modified Bessel function of the first kind, order zero
I_1	- modified Bessel function of the first kind, order one
k	- thermal conductivity, W/mK
K_0	- modified Bessel function of the second kind, order zero
K_1	- modified Bessel function of the second kind, order one
m	- parameter defined by Eqn. 16
n	- parameter defined by Eqns. 17 and 18
N	- total number of elements
q	- heat flux, W/m^2
Q	- heat flow rate, W
r	- radial coordinate
R	- film resistance, K/W
t	- fin thickness, m
T	- temperature, K
z	- axial coordinate

---

rogram Manager

[2]Professor of Mechanical Engineering and Director of MHTL

[3]Packaging Engineer

Greek Symbols

ϕ - axis of rotation
θ - temperature excess, K

Subscripts

e - effective
f_0 - fluid below the fin
f_1 - fluid above the fin
p - pin
s - solid
0 - below the fin
1 - above the fin

INTRODUCTION

The design of microelectronic components and circuit boards has changed radically during the past ten years. Prior to this period, circuit boards were typically populated with widely spaced components, none of which dissipated more than 1 – 2 watts. Maximum localized heat flux densities rarely exceeded 1500 W/m^2 and critical junction temperatures were not approached. However, in recent times the drive to improve signal processing efficiency has resulted in the introduction of many new technologies which allow individual components to be produced that can dissipate up to 8 watts, with heat flux densities exceeding 10,000 W/m^2. The increased thermal load has forced circuit designers to incorporate a variety of imaginative cooling techniques such as the IBM Thermal Conduction Module (TCM) [Blodgett, 1983], the Hewlett-Packard finstrate [HP, 1983], hollow air cooled circuit cards [Laermer, 1974] and numerous heat pipe and immersion cooling techniques. The choice of which cooling technique is most appropriate should be based on a thorough understanding of the thermal network developed between the heat producing components, the circuit board and the cooling medium.

The thermal analysis of electronic and microelectronic equipment dates back to the late 1950's and early 1960's, however most of the information available during this period was obtained empirically and was specific to a given component or circuit board. Several military and company standards [NAVSHIPS, 1955; Walters and Mueller, 1960; and Welsh, 1958 and 1959] served as a "rule of thumb" guide in the design and manufacture of electronic and microelectronic equipment. In the past ten years a greater emphasis has been placed on the development of numerical and analytical techniques for predicting component or junction temperatures, heat flux distributions and heat transfer coefficients. Several authors [David, 1977; Ellison, 1978; Bonnifait et al., 1986] used numerical techniques, such as finite differencing to determine temperature distributions in multilayer circuit boards with isolated or multiple components. The modelling techniques presented in these studies are generally time consuming to set up and require a great deal of computer time for even the simplest of geometries. As an alternative to numerical modelling techniques, the use of purely analytical[Yovanovich, 1986] or a combination of analytical and numerical techniques[Pinto and Mikic, 1986] can offer many advantages especially in applications where multiple, non-similar heat sources are to be modelled or the aspect ratio of the circuit board(length/thickness) is greater than 100.

The following study presents an analytical technique for determining temperature distributions in circular annular geometries. The technique presented is not size dependent, making it equally suitable for assessing heat conduction in large circuit boards or in small device packages. Unlike most techniques for analyzing heat conduction in a cylindrical coordinate system, the analytical model presented allows for *distributed* heat sources on a substrate as shown in Fig. 1.

Two commonly observed examples of a cylindrical heat source with an annular cooling fin are discussed in detail. The first is a typical kovar pin soldered in a through via on a fiberglass/epoxy circuit board, and the second example is a an omni-directional cooling fin. In addition, a hypothetical application with a circular heat source centered on the radial axis at $r = 0$ surrounded by four annular heat sources located at various radial locations is discussed to show the ibility of the modelling technique.

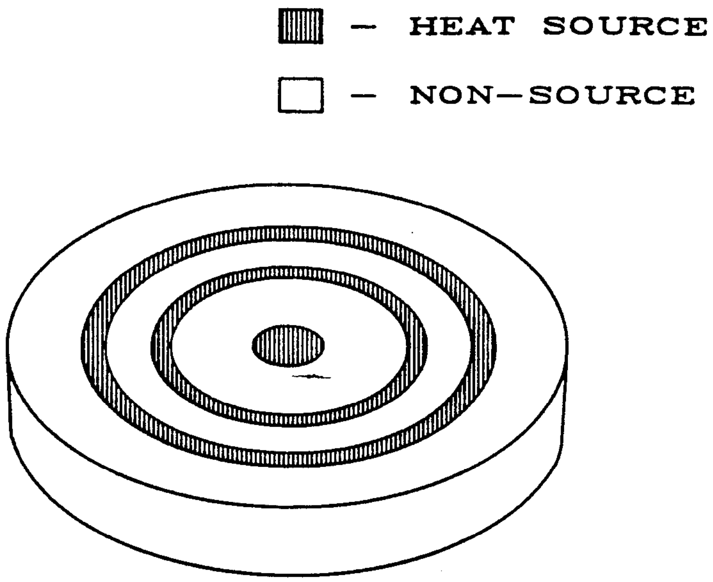

Figure 1: Fin With Distributed Circular and Annular Heat Sources

ANALYTICAL MODEL

Steady-state conduction within an annular fin of thickness t and inner and outer radius a and b where $a < b$, must satisfy the Laplace equation if it is assumed there are no internal heat sources. The two dimensional Laplace equation in cylindrical coordinates is given by

$$\frac{1}{r}\frac{\partial}{\partial r}\left(r\frac{\partial\theta(r,z)}{\partial r}\right)+\frac{\partial^2\theta(r,z)}{\partial z^2}=0 \qquad a\le r\le b, 0\le z\le t \tag{1}$$

which can be expanded to give

$$\frac{\partial^2\theta(r,z)}{\partial r^2}+\frac{1}{r}\frac{\partial\theta(r,z)}{\partial r}+\frac{\partial^2\theta(r,z)}{\partial z^2}=0 \tag{2}$$

where the temperature excess is defined as

$$\theta(r,z)=T_s(r,z)-T_{f_1} \tag{3}$$

Since the thickness of the annular fin is often much smaller than the radius of the fin, it is convenient to assume that heat losses through the ends of the fin are negligible and therefore an adiabatic boundary condition can be imposed over the inner and outer surface of the fin.

$$\frac{\partial\theta(r,z)}{\partial r}=0 \qquad \left.\begin{matrix} r=a \\ r=b \end{matrix}\right\},\ 0\le z\le t \tag{4}$$

Over the planar surface of the annular fin ($z = t$) the boundary conditions vary subject to the locations of the heat sources. The boundary condition at the heat source is a Neumann condition (heat flux specified) and is given by

$$\frac{\partial\theta(r,z)}{\partial z}=\frac{q}{k} \qquad z=t,\ \text{source regions} \tag{5}$$

All non-source regions, both on the upper and lower surface of the fin have a Robin boundary condition (film coefficient specified), given as

$$\begin{aligned}\frac{\partial\theta(r,z)}{\partial z} &= -\frac{h_0}{k}\theta(r,0) \qquad z=0,\ \text{non-source regions} &(6)\\ &= -\frac{h_0}{k}\theta(r,0)+\frac{h_0}{k}(T_{f_0}-T_{f_1}) &(7)\end{aligned}$$

$$\frac{\partial\theta(r,z)}{\partial z} = +\frac{h_1}{k}\theta(r,t) \qquad z = t,\ \text{non-source regions} \tag{8}$$

A full two-dimensional solution to the posed problem is extremely complex because of the non-uniform boundary onditions specified on the planar surfaces of the fin. In some instances the complexity of the two-dimensional problem an be reduced through an examination of the resistive paths both within the solid and at the fluid/solid interface. The i[illegible]mber which is a measure of the internal resistance to heat flow to the external resistance to heat flow is defined s

$$Bi = ht/k_e \tag{9}$$

When the Biot number is less than 0.2 the external resistance is predominant and the internal resistance across the n thickness does not have a significant role in determining temperature distribution. The two-dimensional problem an then be simplified into the form of a one-dimensional problem.

A typical circuit board with an effective thermal conductivity of 5 W/mK and a thickness of 1.6 mm can be modelled s a fin with a resultant Biot number of approximately 0.006 – 0.02 for a range of flow velocities between 1 and 5 m/s.

A solution to the governing differential equation given in Eqn. 2 can be obtained by multiplying each term by dz nd integrating from $z = 0$ to $z = t$.

$$\int_0^t \frac{\partial^2\theta(r,z)}{\partial r^2}dz + \int_0^t \frac{1}{r}\frac{\partial\theta(r,z)}{\partial r}dz + \int_0^t \frac{\partial^2\theta(r,z)}{\partial z^2}dz = 0 \tag{10}$$

Eqn. 10 can be rearranged using Leibnitz's rule to give

$$\frac{\partial^2}{\partial r^2}\int_0^t \theta(r,z)dz + \frac{1}{r}\frac{\partial}{\partial r}\int_0^t \theta(r,z)dz + \frac{\partial\theta(r,t)}{\partial z} - \frac{\partial\theta(r,0)}{\partial z} = 0 \tag{11}$$

But

$$\int_0^t \theta(r,z)dz = t\left(\frac{1}{t}\right)\int_0^t \theta(r,z)dz = t\overline{\theta} \tag{12}$$

w[illegible] $\overline{\theta}$ is the mean cross sectional temperature excess.

Therefore Eqn. 11 becomes

$$t\left\{\frac{\partial^2\overline{\theta}}{\partial r^2} + \frac{1}{r}\frac{\partial\overline{\theta}}{\partial r}\right\} + \frac{\partial\theta(r,t)}{\partial z} - \frac{\partial\theta(r,0)}{\partial z} = 0 \tag{13}$$

Since h_1t/k_e and h_0t/k_e are less than 0.2, the temperature excess at any value of t can be approximated as the mean cross sectional temperature excess

$$\theta(r,0) = \theta(r,t) = \overline{\theta} \tag{14}$$

Thus the governing differential equation is

$$\frac{\partial^2\overline{\theta}}{\partial r^2} + \frac{1}{r}\frac{\partial\overline{\theta}}{\partial r} - m^2\overline{\theta} = -n \tag{15}$$

where

$$m^2 = \frac{h_0 + h_1}{kt}, \quad \text{and} \tag{16}$$

$$n = \frac{h_0(T_{f_0} - T_{f_1})}{kt}, \qquad \text{non-sources} \tag{17}$$

$$n = \frac{q + h_0(T_{f_0} - T_{f_1})}{kt}, \qquad \text{sources} \tag{18}$$

The solution to Eqn. 15 is

$$\overline{\theta}(r) = C_1 I_0(mr) + C_2 K_0(mr) + \frac{n}{m^2} \tag{19}$$

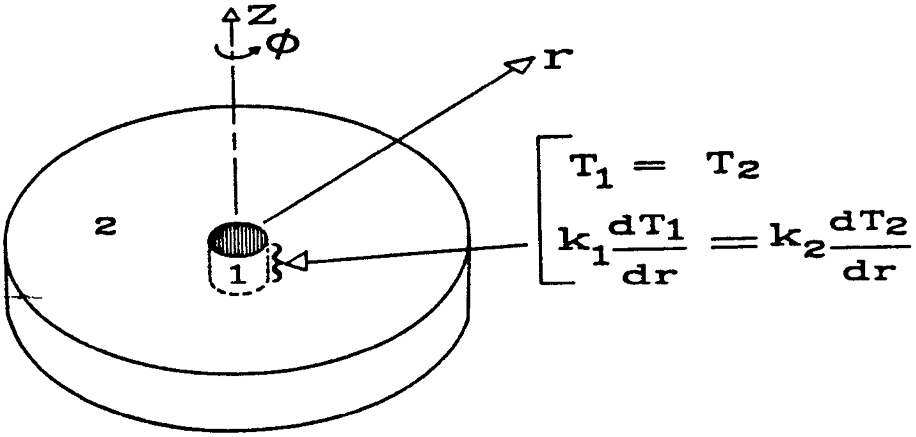

Figure 2: Boundary Conditions Between Adjacent Elements

here C_1 and C_2 are constants of integration. The first two terms of Eqn. 19 are solutions of the homogeneous fferential equation which is Bessel's equation. The functions which appear in Eqn. 19 are modified Bessel functions the first and second kinds of order zero.

A multiple heat source problem can then be formulated by applying Eqn. 19 over each source and non-source region d solving for the constants of integration by applying two boundary conditions at each interior interface as shown Fig.2. If adjacent source and non-source sections are assumed to be in perfect contact, then both the temperature d the product of the temperature gradient and the thermal conductivity can be equated at all interior interfaces as llows

$$\theta(r = b_i) = \theta(r = a_{i+1}) \tag{20}$$

d

$$k_i \frac{d\theta(r = b_i)}{dr} = k_{i+1} \frac{d\theta(r = a_{i+1})}{dr} \tag{21}$$

Combining these boundary conditions with the adiabatic conditions imposed at either end of the fin provides fficient information to solve for all constants of integration. The complete solution for determining the constants of tegration will be presented in [Culham et al., 1987].

The modified Bessel functions of order zero as given in Eqn. 19 and modified Bessel functions of order one which result om applying the boundary conditions must be computed accurately and efficiently in order to obtain the temperature stribution. Routines for calculating the modified Bessel functions I_0, I_1, K_0 and K_1 are given in Appendix I. Further formation on the development of the modified Bessel functions algorithms can be obtained from [Yovanovich, 1986]. he routines are written in IBM-PC-BASIC. Due to the limitation that a positive real number cannot exceed 1.7 x 0^{38}, the maximum Bessel function argument size cannot exceed 88 .

ISCUSSION

The temperature excess at any heat source or non-heat source section of an annular disk can be readily determined om Eqn. 19. If a uniform distribution of the film coefficient or the heat flux is required, the constants of integration d the modified Bessel functions can be determined for each section, and a detailed temperature distribution can be tained by varying the radius accordingly. However, if the film coefficient or the heat flux varies non-uniformly over a ven section, the model can be easily altered to provide discretized elements within each source and non-source section. is assumed that within each element the flux or film coefficient is uniform but by making the element size small ough, the resultant step distribution approaches a continuous distribution. In a fully discretized model, Eqn. 19 must e determined uniquely for each discretized element.

The modified Bessel function of the second kind(K_0) becomes infinite in size in applications where a circular source c[illegible]red at $r = 0$. In this instance the contribution of the term including K_0 must be rejected by setting C_2 to zero.

istributed Sources

Fig. 3 shows an example a circular source centered on the radial axis at $r = 0$ and four annular heat sources l of which are in perfect contact with a circular disk with a radius of 50 mm and a thickness of 1.529 mm. Heat source cations, substrate properties and film coefficients are given in Table 1. The Biot number at the non-source and source cations are 0.184 and 0.092 respectively, which implies that heat conduction can be modelled as one dimensional in ie radial direction.

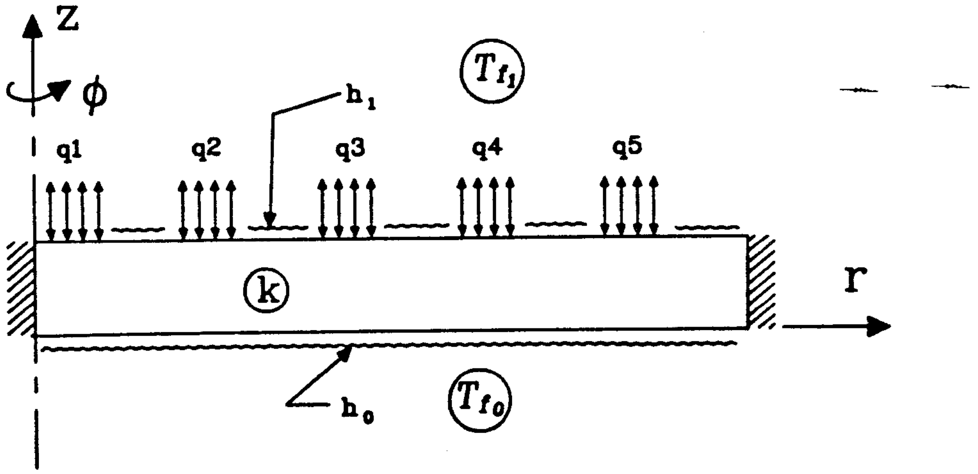

Figure 3: Cross Section of a Circular Annular Fin With Five Discrete Sources

Fig. 4 shows the temperature profile over a radial cross section, where the dimensionless position is given by the ocal radius over the overall outer radius. The choice of heat source flux and source locations has resulted in a situation where the peak source temperature excess at the second, third and fourth sources are approximately identical. As hown in Table 1, the heat input to the outer heat source annuli is substantially greater than the inner annuli, however he cooling area is also greater, offsetting the effect of higher heat input.

Five Heat Source Example

Radial Position mm	Thermal Conductivity W/mK	Heat Flux W/m^2	Heat Flow Rate W	Film Coefficient top W/m^{2}K	Film Coefficient bottom W/m^{2}K
0.0 - 5.0	0.333	5000	0.393	20	20
5.0 - 10.0	0.333			20	20
10.0 - 15.0	0.333	5000	1.964	20	20
15.0 - 20.0	0.333			20	20
20.0 - 25.0	0.333	5000	3.534	20	20
25.0 - 30.0	0.333			20	20
30.0 - 35.0	0.333	5000	5.105	20	20
35.0 - 40.0	0.333			20	20
40.0 - 45.0	0.333	5000	6.676	20	20
45.0 - 50.0	0.333			20	20

Table 1: Thermal conditions for distributed heat source example

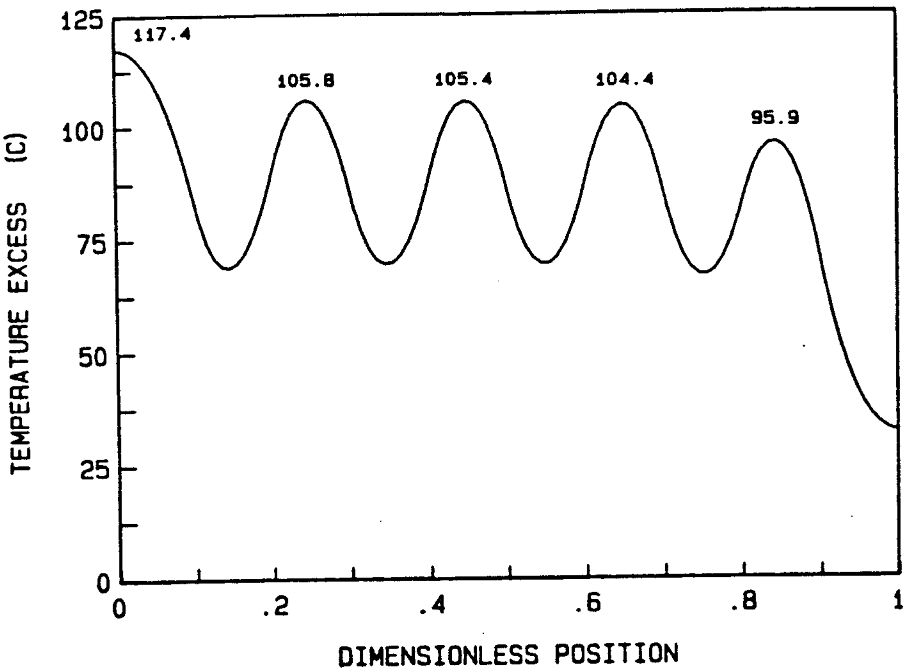

Figure 4: Temperature Distribution Versus Position for a Five Source Fin

Kovar Pin in a Fiberglass/Epoxy Circuit Board

It is often thought that the heat dissipated through the pin of a standard dual inline package is carried directly to the back of the board where it is liberated to the cooling medium. However, a comparison of the thermal resistance of [illegible]kovar pin ($R_p = t/kA$) to the film resistance over the pin at the back surface of the board ($R_{f_0} = 1/hA$), indicates th[illegible]e film resistance is approximately 500 times greater than the resistance of the pin. Heat will fill the pin and then be conducted through the surrounding substrate which has a lower thermal resistance because of its greater surface area exposed to the cooling medium. The heat dissipated directly off the back surface of the pin is only a small fraction of the total heat conducted through the pin. This enables one to model the pin and the surrounding substrate materials as a circular fin with a heat flux imposed over a solid cylinder formed by the kovar pin as shown in Fig. 5.

The outer annulus consists of a fiberglass/epoxy board which is considered to be sheltered by the device package, and therefore has a film coefficient of zero over the upper surface. When a section consists of multiple layers an effective thermal conductivity must be determined by summing the resistance of each layer as if they where thermally connected

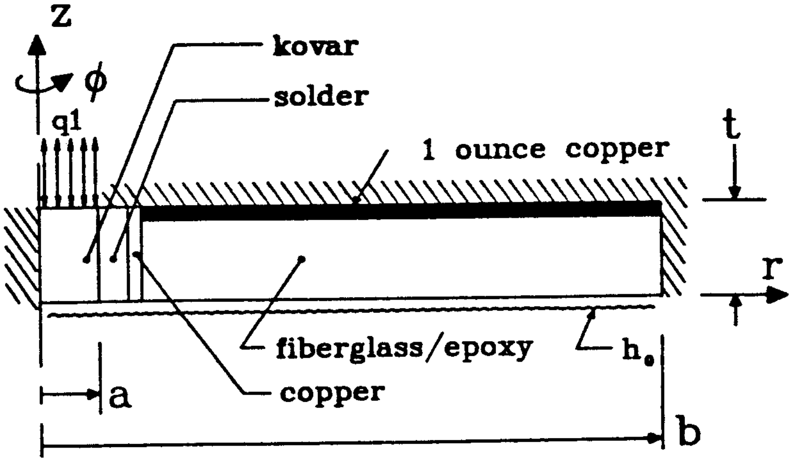

Figure 5: Cross Section of a Through Via in a Fiberglass/Epoxy Circuit Board

parallel. The effective thermal conductivity for a two layer substrate is given as

$$k_e = \frac{k_1 t_1 + k_2 t_2}{t_1 + t_2} \tag{22}$$

model requires the thermophysical properties of each section to be specified individually, allowing the thermal onductivity of the various materials surrounding the pin to be considered.

A fraction of the heat dissipated by the IC is assumed to be conducted through the pin and into the board. Any eat conducted through the air gap between the package and the board is assumed to be negligible.

The solid line profile in Fig. 6 is for an example where the surrounding circuit board is assumed to be a homogeneous omposition of fiberglass and epoxy with the effective thermal conductivity taken as 0.29 W/mK. The temperature emains constant over the pin area and in the solder and copper plate on the interior surface of the via. The temperature alls off quickly in the fiberglass/epoxy section, with a temperature difference of approximately 30 °C between the inner nd outer radius. Even with this temperature drop between the source and the outer radius, the temperature excess t the outer radius of 4 mm remains greater than 40 °C. The thermal conductivity of the fiberglass/epoxy, although elatively low contributes significantly to the dissipation of heat. An analysis which neglects heat conduction within he board because of it's low conductivity can lead to large errors when predicting junction temperatures.

The broken line profile in Fig. 6 is for a configuration similar to the first example but with the addition of a layer f one ounce copper on the fiberglass/epoxy section. The effective thermal conductivity of the board increases by more han 30 times to a value of 9.03 W/mK. This increase in thermal conductivity produces a 36% reduction in the pin emperature through a more effective use of the entire fin area by increasing heat transfer in the radial direction.

Kovar Pin in a Fiberglass/Epoxy Board

Radial Position mm	Material	Thermal Conductivity W/mK	Heat Flux W/m^2	Film Coefficient top W/m^2K	Film Coefficient bottom W/m^2K
0.0000 - 0.2578	kovar	15.64	22600	20	20
0.2578 - 0.3200	solder	67.00	0	20	20
0.3200 - 0.3378	copper	386.00	0	20	20
0.3378 - 4.0000	fiberglass/ epoxy	0.29	0	20	20
	w/ 1 oz. copper	9.03			

Table 2: Thermal conditions for the example of a kovar pin in a fiberglass/epoxy circuit board

mni–Directional Fin

Another example of a circular fin is the omni–directional fin which is sometimes attached to the cap of an IC ackage. A single fin section can be modelled as a circular annular fin as shown in Fig. 7. These fins are typically made f an aluminum alloy which has a thermal conductivity of approximately 180 W/mK. Since the thermal conductivity f both the source and non–source sections is very high, and in turn the Biot number is very small, the fin section pproaches an isothermal condition for most applictions where the fin thickness is greater than one-tenth of a millimeter. wo examples of fins with small fin thickness are presented in Fig. 8. The cross section is sufficiently small so that the emperature excess begins to show the effects of higher localized temperature in the vicinity of where the heat is input nto the fin.

However, the fin thickness of most commercial omni-directional fins is large enough that the temperature distribution ve[illegible]he fin section can be considered isothermal.

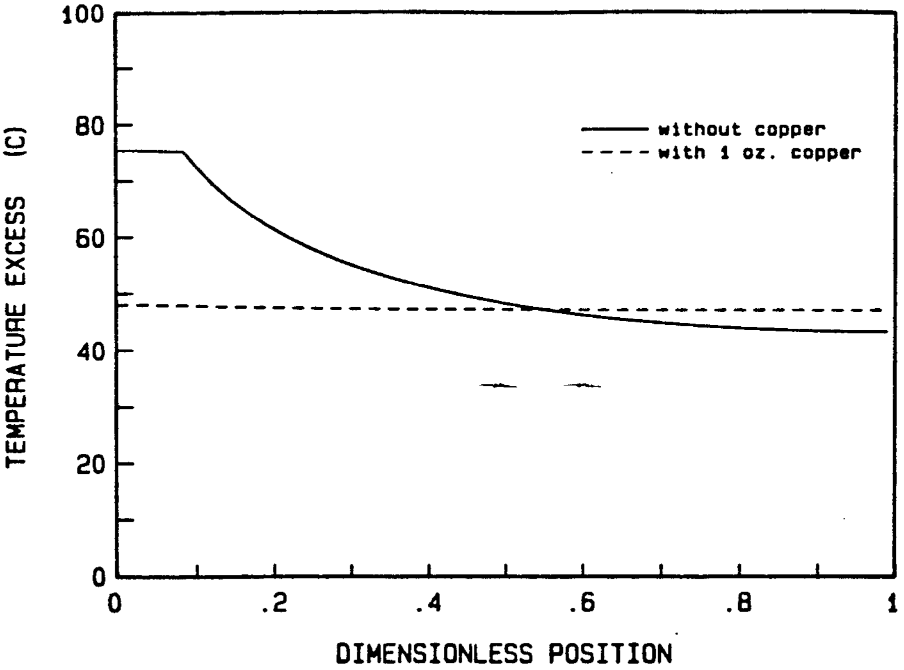

Figure 6: Temperature Distribution Versus Position in the Region Surrounding a Through Via

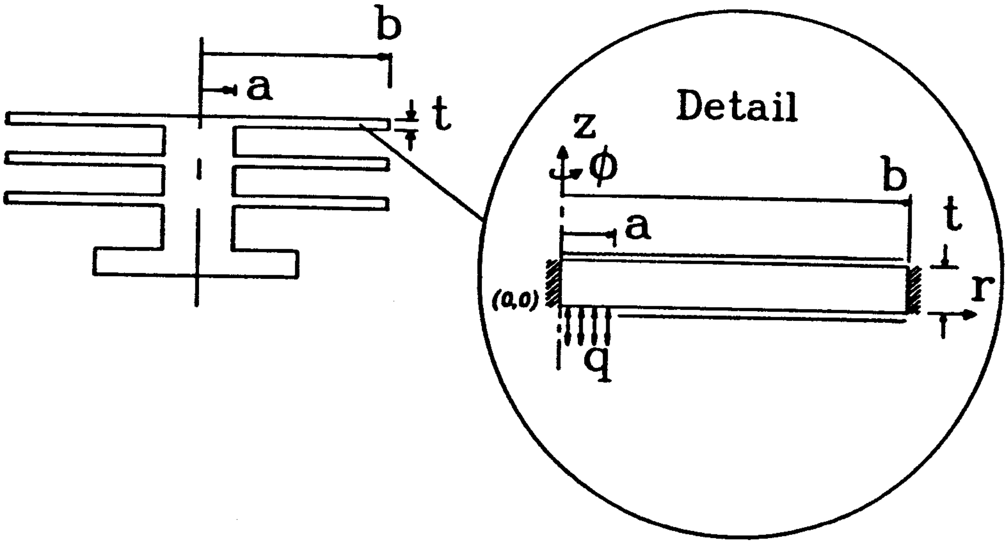

Figure 7: Typical Fin Section of an Omni-Directional Cooling Fin

Omni–Directional Fin					
Radial Position mm	Material	Thermal Conductivity W/mK	Heat Flux W/m^2	Film Coefficient top W/m^{2}K	Film Coefficient bottom W/m^{2}K
0.0000 - 0.0014	aluminum	177	0	20	20
0.0014 - 0.0100	aluminum	177	14614	20	20

Table 3: Thermal conditions for the omni–directional fin example

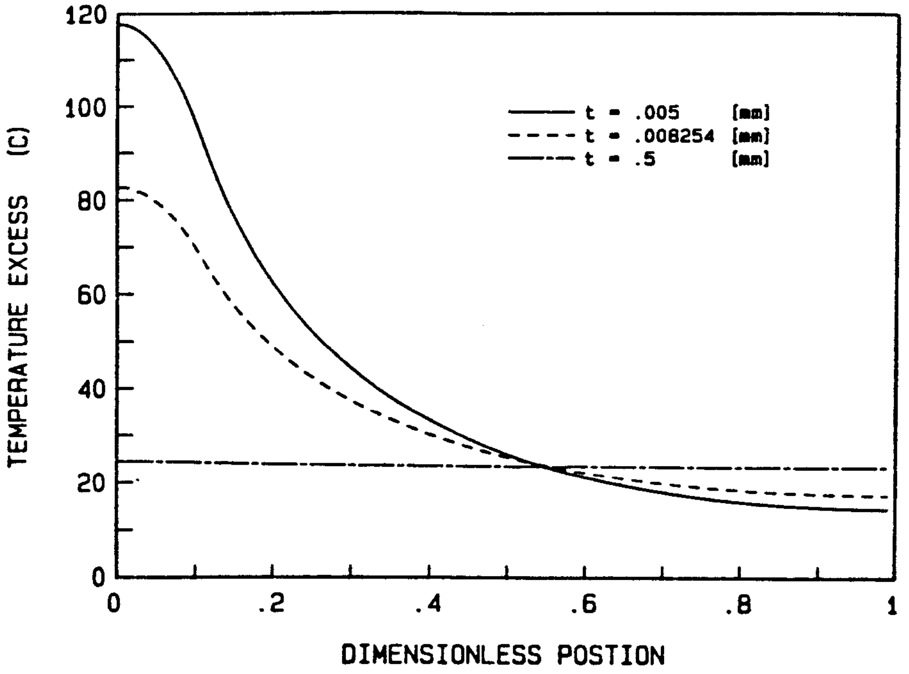

Figure 8: Temperature Distribution Versus Position for an Omni-directional Cooling Fin

eneral Discussion

The temperature distribution for the example of a single isolated heat source at the center of an annular fin, as resented in the kovar pin application can be generalized as shown in Fig. 9 to provide a quick method for determining ie temperature profile within an annular fin without uing the analytical model discussed above. The ordinate in Fig. is a ratio of the localized temperature excess to the temperature excess if the fin were assumed to be isothermal where ie isothermal temperature excess is given as

$$T_{iso} - T_{f_1} = \frac{Q}{hA} \tag{23}$$

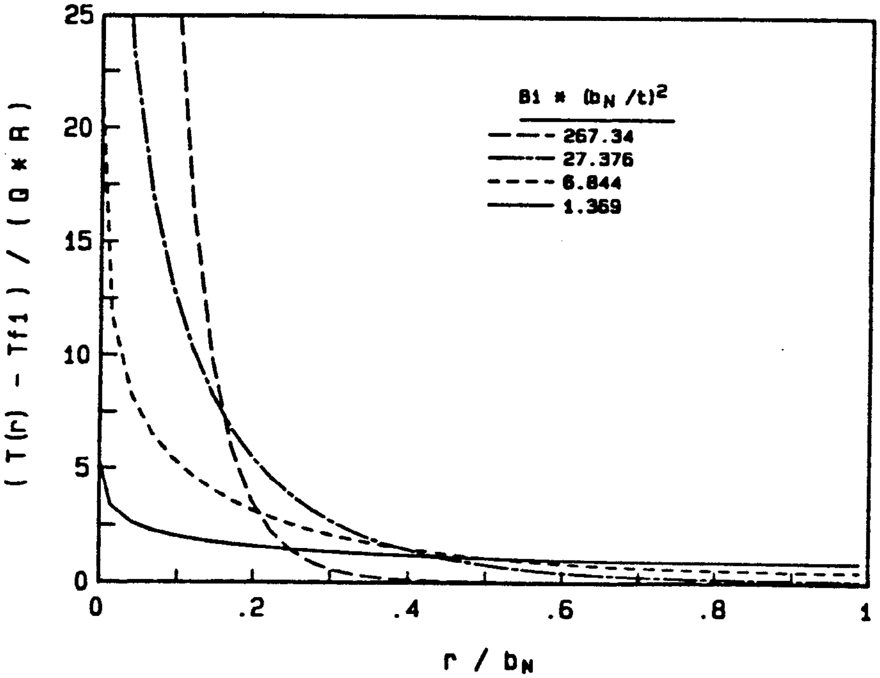

Figure 9: Generalized Temperature Distribution for a Circular Annular Fin with a Single Central Source

d the area – A is the total surface area of the fin.

The four curves in Fig. 9 represent a range of fins with geometric and thermophysical properties that might be ınd in microelectronic applications. The term b_N/t is the aspect ratio of the fin where b_N is the overall outer radius the fin and t is the fin thickness. The Biot number should be calculated in reference to the non-source section of the . The curves are independent of source size, allowing the source temperature and the substrate temperature to be te[illegible]ed for a variety of examples given the Biot number, the source heat flux, the film coefficient and the overall ter radius of the fin. If the Biot number of the source is substantially smaller than the Biot number of the non-source ea, the temperature profile over the source remains relatively constant and then falls off in the non-source region as own in Fig. 6. If the temperature over the source is assumed constant, a line parallel to the abscissa can be drawn, ersecting the appropriate Biot-aspect ratio line at the dimensionless position (r/b_N) corresponding to the source dius. The heat source temperature can then be determined given the film resistance (R = 1/hA) and the source heat w rate (Q). The temperature profile over the annular fin is given by the Biot/aspect ratio line between the source dius and the overall outer radius.

FERENCES

odgett, A.J. Jr., 1983,"Microelectronic Packaging", Scientific American, Vol. 249, No. 1.

nnifait, M., Cadre, M. and Charlier, H., 1986, "Thermal Simulations for Electronic Components Using Finite Elements and Nodal Networks", AIAA/ASME 4th Thermophysics and Heat Transfer Conference, Boston, Massachusetts.

vid, R.F., 1977, "Computerized Thermal Analysis of Hybrid Circuits", IEEE Transactions of Hybrids and Packaging, Volume PHP-13, Number 3.

lison, G.N., 1978, "A Thermal Analysis Computer Program Applicable to a Variety of Microelectronic Devices", Proceedings of the International Microelectronics Symposium, Minneapolis, Minnesota.

wlett-Packard [HP], 1983, "Reshaping 32 – Bit Power: The Astonishing HP 9000 Technology", Trade [illegible]chure.

ermer, L., 1974, "Air Through Hollow Cards Cools High-Power LSI", Electronics, Vol. 47, No. 12.

AVSHIPS, 1955, "Design Manual of Cooling Methods for Electronic Equipment", NAVSHIPS 900-190, Department of the Navy, Bureau of Ships.

nto, E.J. and Mikic, B.B., 1986, "Temperature Prediction on Substrates and Integrated Circuit Chips", AIAA/ASME 4th Thermophysics and Heat Transfer Conference, Boston, Massachusetts.

alters, F.M. and Mueller, R.D., 1960, "Design Manual, Electronic Equipment Environmental Conditioning", Airesearch Manufacturing Company (Garrett Corp.), Report L-5009-R.

elsh, J.P., 1958, "Design Manual of Methods of Forced Air Cooling Electronic Equipment", Cornell Aeronautical Laboratories, Buffalo, New York.

elsh, J.P., 1959. "Handbook of Methods of Cooling Air Force Ground Electronic Equipment", RADC-TR-58-126, Astia No. AD-148907.

vanovich, M.M., Culham, J.R. and Lemczyk, T.F., 1986, "Simplified Analytical Solutions and Numerical Computation of One and Two-Dimensional Circular Fins With Contact Conductance and End Cooling", AIAA 24th Aerospace Sciences Meeting, Reno, Nevada.

ulh[illegible] J.R. and Yovanovich, J.R., 1987, "Non-Iterative Technique for Computing Temperature Distributions in Flat Plates with Distributed Heat Sources and Convective Cooling", Second ASME–JSME Thermal Engineering Joint Conference, Honolulu, Hawaii.

e: I_0
tion: Calculates the modified Bessel function – first kind, order zero for any argument – ARG.
meters Sent: ARG is the value of the argument to be evaluated.
m s Returned: BI0 is the value of the modified Bessel function I_0 (ARG)

```
'=========================================================================
'
'     MODIFIED BESSEL FUNCTION IO
'
PI=3.141592653589793#
IF ARG>35# THEN 1120 ELSE 1060
TERM11=0#
FOR J=1 TO 7
TERM11=TERM11+(EXP(ARG*COS(J*PI/15))+EXP(-ARG*COS(J*PI/15)))/2#
NEXT J
BIO=1#/15#*((EXP(ARG)+EXP(-ARG))/2#+2#*TERM11)
GOTO 1190
TERMIO(0) = 1#
TERMBIO = 0#
FOR J=1 TO 10
TERMIO(J)=(-(2#*J-1)^2/(8#*ARG*J))*TERMIO(J-1)
IF INT(J/2)=J/2 THEN TERMBIO=TERMBIO+TERMIO(J) ELSE TERMBIO=TERMBIO-TERMIO(J)
NEXT J
BIO=(EXP(ARG)/(2#*PI*ARG)^.5)*(1#+TERMBIO)
RETURN
```

e: I_1
ti Calculates the modified Bessel function – first kind, order one for any argument – ARG.
meters Sent: ARG is the value of the argument to be evaluated
meters Returned: BI1 is the value of the modified Bessel function I_1 (ARG)

```
'=========================================================================
'
'    MODIFIED BESSEL FUNCTION I1
'
PI=3.141592653589793#
IF ARG>35# THEN 2120 ELSE 2060
TERM22=0#
FOR J=1 TO 7
TERM22=TERM22+COS(J*PI/15#)*(EXP(ARG*COS(J*PI/15#))-EXP(-ARG*COS(J*PI/15#)))/2#
NEXT J
BI1=1#/15#*((EXP(ARG)-EXP(-ARG))/2#+2#*TERM22)
GOTO 2200
TERMI1(0)=1#
TERMBI1 = 0#
TERMI1(1)=3#/(8#*ARG)
FOR J=2 TO 10
TERMI1(J)=(-((2#*J-1)^2-4)/(8#*ARG*J))*TERMI1(J-1)
IF INT(J/2)=J/2 THEN TERMBI1=TERMBI1+TERMI1(J) ELSE TERMBI1=TERMBI1-TERMI1(J)
NEXT J
BI1=(EXP(ARG)/SQR(2#*PI*ARG))*(1-TERMI1(1)+TERMBI1)
RETURN
```

ame: K_0
unction: Calculates the modified Bessel function – second kind, order zero for any argument – ARG.
arameters Sent: ARG is the value of the argument to be evaluated
arameters Returned: BK0 is the value of the modified Bessel function K_0 (ARG)

```
000 '=====================================================================
010 '
02      MODIFIED BESSEL FUNCTION KO
030 '
040 PI=3.141592653589793#
050 IF ARG>35# THEN 3160
060 X=LOG(1D+17)/ARG
070 A=LOG(X+SQR(X*X -1#))
080 M=INT(A)+17
090 TERM1=EXP(-ARG)+EXP(-ARG*((EXP(A)+EXP(-A))/2#))
100 TERM2=0#
110 FOR J=1 TO M-1
120 TERM2=TERM2+EXP(-ARG*((EXP(J*A/M)+EXP(-J*A/M))/2#))
130 NEXT J
140 BKO=(.5#*TERM1+TERM2)*A/M
150 GOTO 3220
160 TERMKO(0)=1#:TERMBKO=1#
170 FOR J=1 TO 10
180 TERMKO(J)=(-(2#*J-1)^2)/(8#*ARG*J)*TERMKO(J-1)
190 TERMBKO=TERMBKO+TERMKO(J)
200 NEXT J
210 BKO=SQR(PI/(2#*ARG))*EXP(-ARG)*TERMBKO
220 RETURN
```

ame: K_1
unction: Calculates the modified Bessel function – second kind, order one for any argument – ARG.
ar[illegible]ters Sent: ARG is the value of the argument to be evaluated
ara[illegible]eters Returned: BK1 is the value of the modified Bessel function K_1 (ARG)

```
000 '====================================================================
010 '
020 '    MODIFIED BESSEL FUNCTION K1
030 '
040 PI=3.141592653589793#
050 IF ARG>35# THEN 4160
060 X = LOG(1D+17)/ARG
070 A = LOG(X+SQR(X*X-1#))
080 M = INT(A)+17
090 TERM1=EXP(-ARG)+((EXP(A)+EXP(-A))/2#)*EXP(-ARG*((EXP(A)+EXP(-A))/2#))
100 TERM2=0#
110 FOR J=1 TO M-1
120 TERM2=TERM2+((EXP(J*A/M)+EXP(-J*A/M))/2#)*EXP(-ARG*((EXP(J*A/M)+EXP(-J*A/M))/2#))
130 NEXT J
140 BK1=((.5*TERM1)+TERM2)*A/M
150 GOTO 4220
160 TERMK1(0)=1#:TERMBK1=1#
170 FOR J=1 TO 10
80 TERMK1(J)=(4#-(2#*J-1)^2)/(8#*ARG*J)*TERMK1(J-1)
90 TERMBK1=TERMBK1+TERMK1(J)
200 NEXT J
21[illegible]1=SQR(PI/(2#*ARG))*EXP(-ARG)*TERMBK1
20 RETURN
```

KNOWLEDGEMENTS

The authors acknowledge the financial support of the Natural Sciences and Engineering Research Council under AI[illegible]rating grant P-8322 for support under the University-Industry Program. The authors also wish to acknowledge Fas[illegible] and J. Sheaff for their efforts in preparing the figures presented in this paper.